

Emulation of Operational Amplifiers and Diodes in Audio Distortion Circuits

Rafael C. D. Paiva, Stefano D'Angelo, Jyri Pakarinen, and Vesa Välimäki, *Senior Member, IEEE*

Abstract—This brief presents a generic model to emulate distortion circuits using operational amplifiers and diodes. Distortion circuits are widely used for enhancing the sound of guitars and other musical instruments. This brief introduces a new model for an ideal operational amplifier that does not include implicit equations and is thus suitable for implementation using wave digital filters (WDFs). Furthermore, a novel WDF model for a diode is proposed using the Lambert W function. A comparison of output signals of the proposed models to those obtained from a reference simulation using SPICE shows that the distortion characteristics are accurately reproduced over a wide frequency range. Additionally, the proposed model enables real-time emulation of distortion circuits using ten multiplications, 22 additions, and two interpolations from a lookup table per output sample.

Index Terms—Acoustic signal processing, circuit simulation, harmonic distortion, music, nonlinear systems.

I. INTRODUCTION

RECENT advances in audio signal processing have included the real-time emulation of analog nonlinear circuits using digital techniques [1]–[3]. These techniques are important for the development of new products that preserve the timbre of vintage audio equipment at low cost. These include portable effect boxes for electric guitars, the bass, and other musical instruments; real-time effect processing software; and music synthesis in games. Hence, this kind of effect requires low computational cost for being feasible in real time.

Several studies have been presented for modeling this type of equipment [1]. The models include black-box approaches [4]–[6], which are good when there is no physical knowledge of the system being modeled, and physical models. Physical models include physically informed models [7]–[9], state space methods [10]–[12], and the K -method [13]–[15]. However, this type of solution often requires deriving the system equations, making the models laborious to implement. Additionally, some of these solutions require iterative methods or matrix inversions, which may increase the complexity of real-time systems.

Another class of solutions emerges from using wave digital filters (WDF), which can be computed in a block-oriented approach [2], [16]–[18]. Examples of WDF implementations include a guitar-distortion vacuum-tube amplifier model [19], [20], a diode clipper [21], and an audio transformer model [22]. With WDFs, computing the response of circuits with simple nonlinearity without matrix inversion or iterative methods is possible, leading to complexity that increases linearly with the number of simulated components $\mathcal{O}(N)$.

A significant fraction of guitar distortion effects employs operational amplifiers and diodes. Additionally, a multitude of audio effects emerges from the use of operational amplifiers and diodes, which include several ring modulators, analog octavers, and others. Previous studies have shown models for this class of circuits derived from physically informed models [8] and state space equations [10]. Moreover, an analog oscillator circuit used for synthesis is modeled with WDFs in [2]. However, in all these cases, the models are derived for specific circuits, and they are not easily generalized for other distortion circuits used in music.

The objective of this brief is to derive a new model for traditional operational amplifier circuits used in guitar distortion. The model is easily applicable to most operational amplifier circuits used in effects for musical instruments and is suitable for real-time application.

This brief is organized as follows. Section II introduces a new model of an ideal operational amplifier. The derivation of a closed-form formula to simulate a diode in the wave digital domain is given in Section III. The validation of the proposed model is presented in Section IV, and the computational cost of the model is analyzed in Section V. Finally, Section VI concludes this brief.

II. OPERATIONAL AMPLIFIER MODEL

A circuit using an operational amplifier is shown in Fig. 1(a). In its predominant application, operational amplifiers are used to build general-purpose voltage amplifiers or filters. In the inverting amplifier configuration, a voltage is applied to the terminal V_{i0} , and the gain is given by the ratio of impedance as $A = -Z_f/Z_0$ [23]. On the other hand, in the noninverting amplifier configuration a voltage is applied to the terminal V_{i1} and the gain is given by $A = Z_f/(Z_0 + Z_f)$ [23]. Additionally, a frequency-dependent gain is obtained when using a reactive component, such as a capacitor, in Z_f or Z_0 .

A traditional model of the operational amplifier that uses a voltage-controlled voltage source is shown in Fig. 1(b). This model has only a few components and is able to reproduce the

Manuscript received March 27, 2012; revised June 6, 2012; accepted August 4, 2012. Date of publication September 21, 2012; date of current version October 12, 2012. This work was supported in part by the Centre for International Mobility and in part by Nokia Foundation. This brief was recommended by Associate Editor R. Martins.

R. C. D. Paiva is with the Department of Signal Processing and Acoustics, Aalto University School of Electrical Engineering, 00076 Espoo, Finland, and also with the Nokia Institute of Technology, INdT, 69093-415 Manaus, Brazil.

S. D'Angelo and V. Välimäki are with the Department of Signal Processing and Acoustics, Aalto University School of Electrical Engineering, 00076 Espoo, Finland.

J. Pakarinen is with the Dolby Laboratories, 113 30 Stockholm, Sweden.
Digital Object Identifier 10.1109/TCSII.2012.2213358

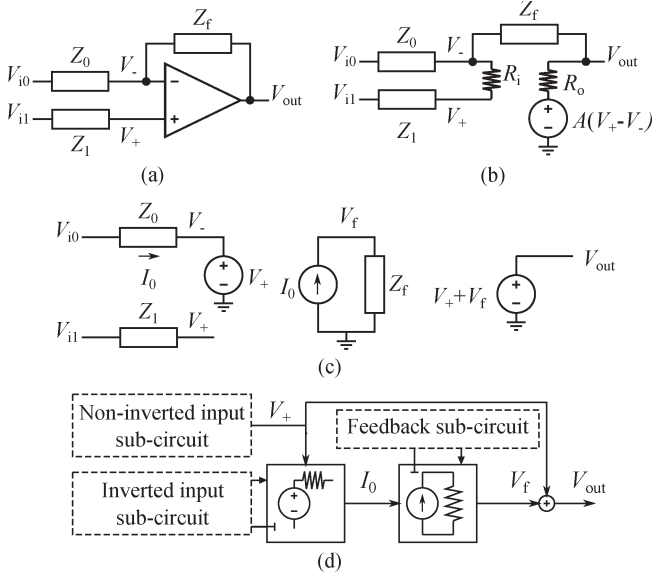


Fig. 1. (a) Typical operational amplifier connections and models based on input-output behavior: (b) Traditional model [23]. (c) Simplified circuit model. (d) WDF model for operational amplifiers.

behavior of different circuits using operational amplifiers. However, the voltage source used in this model has instantaneous dependence on other voltages in the circuit, causing the solution for the circuit using this model to involve implicit equations. They are typically avoided when implementing real-time audio effects since they require computationally heavy operations, such as a matrix inversion or iterative methods.

A simplified model of an operational amplifier circuit can be obtained by analyzing the characteristics of ideal amplifiers. First, the ideal operational amplifier has an infinite gain for the voltage difference between the nodes V_- and V_+ . Hence, due to the infinite gain of the ideal amplifier, in practical circuits the voltage difference between its input nodes is nearly zero, i.e., $V_- \approx V_+$. Second, the ideal operational amplifier has very low output impedance, which makes the output voltage of the operational amplifier circuit independent of the impedance that it is connected to.

Thus, by applying the Kirchhoff voltage law to the circuit in Fig. 1(a), the output voltage is the sum of the voltage at node $-$, i.e., V_- , and the voltage across the impedance Z_f . This fact is used in the model of Fig. 1(c), by making $V_{out} = V_+ + V_f$. Additionally, ideal operational amplifiers have an infinite input impedance, and no current flows into it from the input nodes $-$ and $+$. This implies that the current through Z_1 is zero and that the voltage at node $-$ is controlled by the voltage at node $+$. This fact is mapped into the model in Fig. 1(c) by connecting a voltage-controlled voltage source at node $-$. Finally, the current I_0 through the impedance Z_0 can only flow through impedance Z_f , which is modeled in Fig. 1(c), connecting a current source controlled by I_0 in parallel to Z_f .

The model in Fig. 1(c) is mapped onto the equivalent WDF model in Fig. 1(d). In the WDF model, only two components are needed to model the operational amplifier. Nonideal voltage and current sources are used in order to allow for a reflection-free WDF implementation of the current-voltage sources.

Using the general WDF model in Fig. 1(d), various audio circuits having negative feedback can be emulated.

III. DIODE MODEL

The exact closed-form analytical solution for the current flowing through a diode with a series resistance involves the Lambert W function [24]. This section shows that the same holds true for the WDF model of a single diode. Additionally, this result is used to develop a WDF model of two identical and antiparallel diodes.

The Shockley large-signal model relates the diode current I through a p-n junction diode to the diode voltage V across as

$$I = I_S \left(e^{\frac{V}{n_D V_T}} - 1 \right) \quad (1)$$

where I_S is the saturation current or scale current of the diode, V_T is the thermal voltage, and n_D is the diode ideality factor.

In order to emulate the diode using WDFs, a closed-form formula is desirable to compute the wave variables. The mapping to the wave digital domain is accomplished using the wave transformation as

$$V = \frac{a+b}{2}, I = \frac{a-b}{2R_P} \quad (2)$$

where V and I are the voltage and current of the component, respectively; a and b are the incoming and outgoing wave variables in the wave domain, respectively; and R_P is the port resistance [16]. The expression desired is a nonlinear function with which the output wave of a diode can be readily obtained as $b = f(a, R_P, I_S, n, V_T)$. Substituting (2) in (1) gives

$$e^{\frac{a+b}{2n_D V_T}} = \frac{a-b}{2R_P I_S} + 1 \quad (3)$$

which can be solved for b using the Lambert W function $W()$ as follows:

$$b = f(a, R_P, I_S, n_D, V_T) = a + 2R_P I_S - 2n_D V_T W \left(\frac{R_P I_S}{n_D V_T} e^{\frac{R_P I_S + a}{n_D V_T}} \right). \quad (4)$$

Audio distortion circuits often use two antiparallel diodes. In a practical simulation, they can be combined in a single nonlinear element [10]. In this case, (1) is modified as

$$I = I_S \left[\left(e^{\frac{V}{n_D V_T}} - 1 \right) - \left(e^{-\frac{V}{n_D V_T}} - 1 \right) \right]. \quad (5)$$

If only one diode is considered to conduct, i.e., the forward current is much higher than the reverse current of the other diode, one can assume that

$$e^{\frac{|V|}{n_D V_T}} - 1 \gg e^{-\frac{|V|}{n_D V_T}} - 1 \quad (6)$$

which leads to the nonlinear wave mapping for two identical antiparallel diodes as follows:

$$b = \text{sgn}(a) f(|a|, R_P, I_S, n_D, V_T) \quad (7)$$

where $\text{sgn}(x)$ is the signum function.

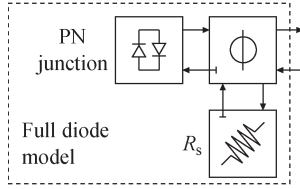


Fig. 2. WDF diode model including a p-n junction and series resistance.

A fast approximation of the Lambert W function is desirable for the emulation of distortion circuits. In this brief, the approximation is based on an iterative process, where an improved approximation $W_{k+1}(x)$ is calculated based on a previous one $W_k(x)$ as [25]

$$W_{k+1}(x) = \begin{cases} \ln \frac{x}{W_k(x)}, & \text{if } x \geq e, \\ x e^{-W_k(x)}, & \text{if } x < e, \end{cases} \quad (8)$$

where $e \approx 2.7182$ is the base of the natural logarithm. The initial value of $W(x)$ is obtained by linear interpolation of values from a lookup table. A lookup table containing 8000 values logarithmically spaced between 10^{-24} and 10^{300} has been verified to yield sufficient accuracy.

In addition to the p-n junction behavior, real diodes are also described by their series resistance R_s . This resistance is responsible for an additional voltage drop across the diode terminals. Hence, the WDF model for a diode with a series resistor is obtained by combining a p-n junction model, obtained from (7), and a resistor with a series adaptor as in Fig. 2.

IV. SIMULATION RESULTS

In this section, simulation results are used to validate the proposed model. For that purpose, the WDF model was compared with reference simulation results obtained with a SPICE-based software LTSpice [26].

The diode model was evaluated individually in a simulation where a $10\text{-}\mu\text{A}$ sinusoidal current source is connected to two antiparallel diodes, and the resulting voltage was evaluated. A low input frequency of 0.5 Hz was used because the diode model in SPICE has a small capacitance. Additionally, a parallel resistance of $1\text{ M}\Omega$ is connected to the current source. This circuit uses two 1N914 diodes, with series resistance $R_s = 0.568\text{ }\Omega$ and the parameters for the Shockley equation are $I_S = 2.52\text{ nA}$, $n_D = 1.752$, and $V_T = 25.86\text{ mV}$.

Fig. 3(a) shows the evaluation of the percentual error as a function of the diode current, where the error is larger for small current values. One reason for the error at low diode currents is that the reverse diode current was neglected in (6). However, real guitar distortion circuits often use a resistor connected in parallel with the diodes, whose current is higher than the diode current, causing the diode function error to be negligible. Additionally, Fig. 3(a) shows that using one iteration of the Lambert W function approximation yields practically the same error as using two, which indicates that increasing the number of iterations is unnecessary. Fig. 3(b) shows the distortion error for each harmonic, which is smaller than 0.15 dB with all approximations. This indicates that the 8000-point lookup table

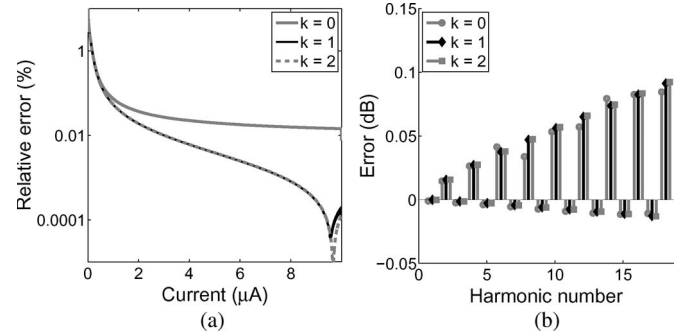


Fig. 3. Evaluation of the diode model for $k = 0, 1$, and 2 iterations for the Lambert W function approximation with a sinusoidal input. (a) Voltage approximation error as a function of the diode current. (b) Error for approximating individual harmonics.

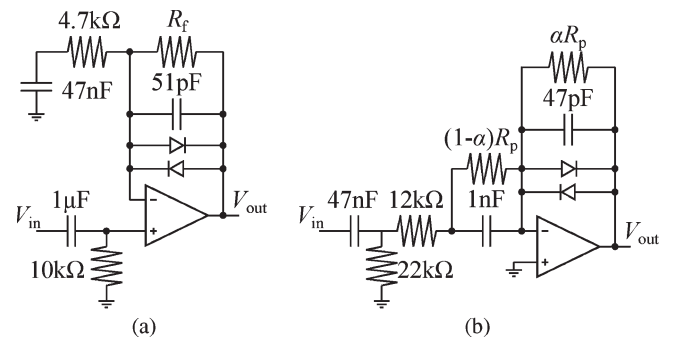


Fig. 4. Distortion circuits used in the simulations. (a) Noninverting distortion [5]. (b) Inverting distortion [10].

provides good accuracy for the Lambert W function without the need for further iterations.

Two typical distortion circuits using both operational amplifiers and diodes were evaluated. One circuit uses a noninverting amplifier configuration, as shown in Fig. 4(a), whereas the other uses an inverting amplifier configuration, shown in Fig. 4(b).

The first evaluated circuit, shown in Fig. 4(a), is used in some versions of the Tube Screamer guitar effect. The distortion of this circuit is controlled by the resistance R_f , which was kept at the constant value of $R_f = 500\text{ k}\Omega$ during the simulations, yielding a total harmonic distortion (THD) of 5.7% at 1000 Hz . The simulated circuit has two 1N914 diodes, with the other parameters described in Fig. 5(a). The WDF implementation of this circuit is presented in Fig. 5(a). This implementation includes the cascaded computation of three subcircuits based on the model in Fig. 1(d). The first one is used to calculate the voltage at input 1 of the operational amplifier. The second one uses this voltage to determine the current at impedance Z_0 , whereas the third uses this current to determine the voltage at the feedback impedance. The output voltage is thus the sum of the voltage at input 1 and at the feedback impedance.

The second circuit, shown in Fig. 4(b), is based on Marshall preamplifiers [10], such as in the 4100 JCM900 Hi Gain Dual Reverb head. In the simulation results, the distortion gain was constant, with $\alpha = 0.999$ and $R_p = 220\text{ k}\Omega$. This circuit uses two NSCW100 diodes, which are simulated with the series resistance $R_s = 8.163\text{ }\Omega$ and the parameters for the Shockley equation $I_S = 16.88\text{ nA}$, $n_D = 9.626$, and $V_T = 25.85\text{ mV}$, yielding a THD of 11% at 1000 Hz . The WDF network based

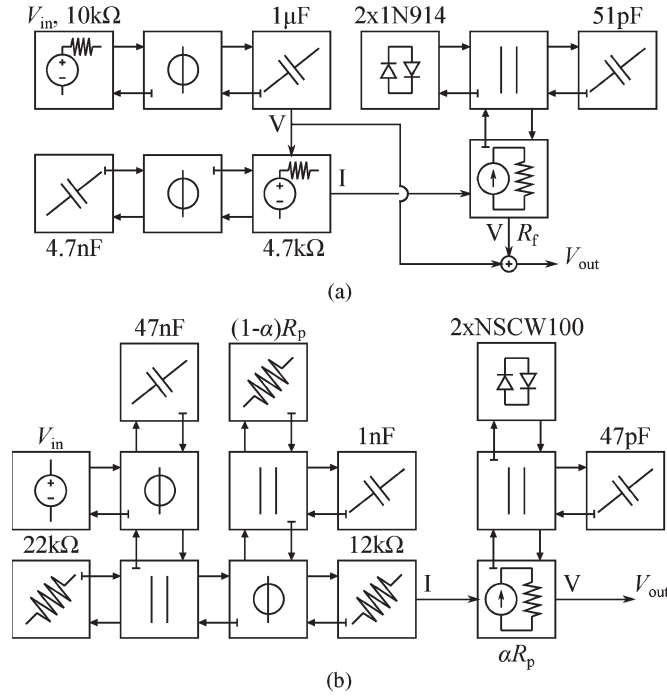


Fig. 5. WDF models for the circuits in Fig. 4: (a) noninverting and (b) inverting distortion.

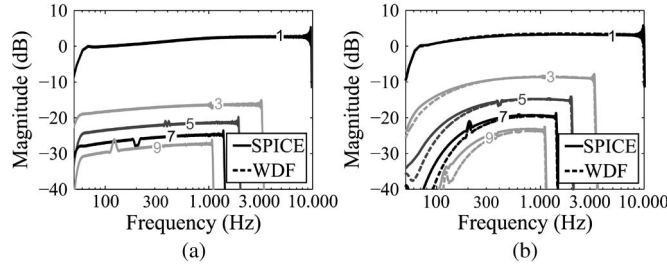


Fig. 6. Swept-sine results for the model in SPICE [26] and using the proposed WDF model. (a) Results for the noninverting configuration in Fig. 4(a). (b) Results for the inverting configuration in Fig. 4(b).

on the model of Fig. 1(d) is presented in Fig. 5(b). This structure uses only two cascaded subcircuits, whereas the one in Fig. 5(a) uses three. The number of subcircuits is decreased for this example because it uses an inverter configuration, and the input of the operational amplifier is grounded.

The simulation results are shown in Fig. 6 for the swept-sine analysis [27] using Pakarinen's Distortion Analysis Toolkit [28] with a 1-s long signal with frequencies between 50 and 10 000 Hz and a sampling frequency of 96 kHz. The results for the noninverting configuration are shown in Fig. 6(a). The frequency response of all the observed odd harmonics up to the ninth harmonic is in nearly perfect agreement with the reference results.

The inverting configuration is analyzed in Fig. 6(b). In this configuration, the amplitude of the harmonic components can be observed to increase with the fundamental frequency of the input. The same behavior is observed with the proposed WDF implementation, where some deviation from the SPICE reference simulation can be noticed for low amplitudes of each harmonic component at low frequencies. However, informal listening tests have revealed no perceptual differences between

TABLE I
COMPUTATIONAL COMPLEXITY PER OUTPUT SAMPLE

	Mult.	Add.	Lamb. W	Exp
Diode model	4	6	1	1
WDF adaptor	1	4	0	0
WDF adapted source	1	0	0	0
WDF non-adapted source	1	1	0	0
Noninverting distortion	10	18	1	1
Inverting distortion	10	22	1	1

the proposed WDF model and the SPICE reference simulation. In both configurations, the energy of the even harmonics was negligible when compared with the odd harmonics and, hence, were omitted from the results.

V. COMPUTATIONAL COST

The complexity of the proposed method is determined by the complexity of implementing the WDF components and the complexity of the diode nonlinear function. The analysis presented in this section considers the number of operations needed per sample and ignores multiplications/divisions that are common for all input samples.

The complexity for the nonlinear function approximation is given as follows. The Lambert W function's first approximation using a lookup table consists of a sorted list search, one multiplication, and one addition for the linear interpolation. The sorted list binary search is implemented with $\mathcal{O}(\log N)$ memory accesses and logical operations, where N is the size of the list. The list described in Section III has 8000 elements. Additionally, each iteration of the Lambert W function approximation requires either one division and one logarithm operation, or one multiplication and one exponential operation. Finally, three multiplications, three additions, and one exponential operation are needed for (7). The exponential function evaluation is usually implemented with a linearly interpolated lookup table.

The complexity of the WDF networks of Fig. 5 may be determined by analyzing the individual components. Adapted resistors require no operations, whereas adapted capacitors require one memory unit to implement the unit delay. The complexity for adapted voltage sources comprises one multiplication, whereas a nonadapted voltage/current source comprises one multiplication and one addition [16], [29]. The complexity for three-port adaptors implies one multiplication and four additions [30].

The resulting complexity for the circuit models in Fig. 5 is shown in Table I. The noninverting configuration of Fig. 5(a) is composed of one diode model, three adaptors, two adapted sources, and one nonadapted source. The inverting configuration comprises four adaptors, one nonadapted source, one adapted source, and one diode model. For example, the inverting distortion circuit of Fig. 5(b) can be implemented with a WDF model, which requires ten multiplications, 22 additions, a Lambert W function evaluation, and one exponential function evaluation per output sample. The inverting distortion circuit implemented in [10] requires 23 multiplications, 18 additions, and one sinh function evaluation, and the solution of an implicit nonlinear equation. This complexity considers the matrix multiplications of their model and ignores the multiplications

by zero. Hence, the proposed solution reduces by 20% the number of floating point operations when the implicit nonlinear equation of [10] is not considered.

VI. CONCLUSION

This brief has introduced a solution to emulate operational amplifier circuits including diodes in virtual analog audio processing. In this solution, a new operational amplifier model is proposed. This modeling approach assumes ideal operational amplifiers and avoids implicit equations. This simplifying assumption reduces the complexity of the model, enabling easy application with WDFs.

Moreover, a new closed-form solution is proposed to model diodes in the wave digital domain. This solution applies the Lambert W function, and an approximation with reduced complexity is presented, where a relatively small lookup table can accurately approximate this function for the diode model.

The proposed method shows that it is possible to emulate guitar distortion in real time with a small number of mathematical operations. The model requires about ten multiplications, 20 additions, one Lambert W function evaluation, and one exponential operation per sample if no iteration is used, which makes it suitable for real-time effects. Additionally, this model may be used in other digital systems that require real-time or fast simulation of this type of circuit.

In order to prove the accuracy of the model, simulation results for two circuits were presented. The circuits use the inverting and noninverting operational amplifier connections with diodes in the feedback impedance. The simulation results were compared with results obtained using a reference SPICE simulator. The comparison shows nearly perfect agreement for the noninverting circuit, whereas the inverting circuit had some difference in its low-frequency behavior. An informal listening test revealed that the differences between the proposed model and the reference simulations are not perceived. Both circuits cover a wide range of guitar distortion circuits and strongly support the generality of the model for simulating various distortion circuits used in music. Supplementary material to this brief, including sound examples, can be accessed at <http://www.acoustics.hut.fi/publications/papers/ieeecs-2012-opamp/>.

REFERENCES

- [1] J. Pakarinen and D. T. Yeh, "A review of digital techniques for modeling vacuum-tube guitar amplifiers," *Comput. Music J.*, vol. 33, no. 2, pp. 85–100, Summer 2009.
- [2] G. De Sanctis and A. Sarti, "Virtual analog modeling in the wave-digital domain," *IEEE Trans. Audio, Speech, Lang. Process.*, vol. 18, no. 4, pp. 715–727, May 2010.
- [3] V. Välimäki, S. Bilbao, J. O. Smith, J. Abel, J. Pakarinen, and D. Berners, "Virtual analog effects," in *DAFX—Digital Audio Effects*, U. Zölzer, Ed., 2nd ed. Wiley, 2011, ch. 12, pp. 473–522.
- [4] T. Hélie, "Volterra series and state transformation for real-time simulations of audio circuits including saturations: Application to the Moog ladder filter," *IEEE Trans. Audio, Speech, Lang. Process.*, vol. 18, no. 4, pp. 747–759, May 2010.
- [5] A. Novák, L. Simon, and P. Lotton, "Analysis, synthesis, and classification of nonlinear systems using synchronized swept-sine method for audio effects," *EURASIP J. Adv. Signal Process.*, vol. 2010, pp. 1–8, Feb. 2010.
- [6] R. C. D. Paiva, J. Pakarinen, and V. Välimäki, "Reduced-complexity modeling of high-order nonlinear audio systems using swept-sine and principal component analysis," in *Proc. 45th Audio Eng. Soc. Conf.*, Espoo, Finland, Mar. 2012, pp. 1–10.
- [7] A. Huovilainen, "Non-linear digital implementation of the Moog ladder filter," in *Proc. Int. Conf. Digital Audio Effects*, Naples, Italy, 2004, pp. 61–64.
- [8] D. Yeh, J. Abel, and J. Smith, "Simplified, physically-informed models of distortion and overdrive guitar effects pedals," in *Proc. Int. Conf. Digital Audio Effects*, Bordeaux, France, Sep. 2007, pp. 189–196.
- [9] J. Parker, "A simple digital model of the diode-based ring-modulator," in *Proc. Int. Conf. Digital Audio Effects*, Paris, France, Sep. 2011, pp. 163–166.
- [10] K. Dempwolf, M. Holters, and U. Zölzer, "Discretization of parametric analog circuits for real-time simulations," in *Proc. Int. Conf. Digital Audio Effects*, Graz, Austria, Sep. 2010, pp. 42–49.
- [11] I. Cohen and T. Hélie, "Real-time simulation of a guitar power amplifier," in *Proc. Int. Conf. Digital Audio Effects*, Graz, Austria, Sep. 2010, pp. 30–34.
- [12] F. Fontana and M. Civolani, "Modeling of the EMS VCS3 voltage-controlled filter as a nonlinear filter network," *IEEE Trans. Audio, Speech, Lang. Process.*, vol. 18, no. 4, pp. 760–772, May 2010.
- [13] G. Borin, G. De Poli, and D. Rocchesso, "Elimination of delay-free loops in discrete-time models of nonlinear acoustic systems," *IEEE Trans. Speech Audio Process.*, vol. 8, no. 5, pp. 597–605, Sep. 2000.
- [14] D. Yeh, J. Abel, and J. Smith, "Automated physical modeling of nonlinear audio circuits for real-time audio effects—Part I: Theoretical development," *IEEE Trans. Audio, Speech, Language Process.*, vol. 18, no. 4, pp. 728–737, May 2010.
- [15] D. Yeh, "Automated physical modeling of nonlinear audio circuits for real-time audio effects—Part II: BJT and vacuum tube examples," *IEEE Trans. Audio, Speech, Lang. Process.*, vol. 20, no. 4, pp. 1207–1216, May 2012.
- [16] V. Välimäki, J. Pakarinen, C. Erkut, and M. Karjalainen, "Discrete-time modelling of musical instruments," *Rep. Progr. Phys.*, vol. 69, no. 1, pp. 1–78, Jan. 2006.
- [17] A. Sarti and G. De Sanctis, "Systematic methods for the implementation of nonlinear wave-digital structures," *IEEE Trans. Circuits Syst. I, Reg. Papers*, vol. 56, no. 2, pp. 460–472, Feb. 2009.
- [18] S. Petrusch and R. Rabenstein, "Interconnection of state space structures and wave digital filters," *IEEE Trans. Circuits Syst. II, Exp. Briefs*, vol. 52, no. 2, pp. 90–93, Feb. 2005.
- [19] J. Pakarinen, M. Tikander, and M. Karjalainen, "Wave digital modeling of the output chain of a vacuum-tube amplifier," in *Proc. Int. Conf. Digit. Audio Effects*, Como, Italy, Sep. 2009, pp. 55–59.
- [20] J. Pakarinen and M. Karjalainen, "Enhanced wave digital triode model for real-time tube amplifier emulation," *IEEE Trans. Audio, Speech, Lang. Process.*, vol. 18, no. 4, pp. 738–746, May 2010.
- [21] D. T. Yeh and J. O. Smith, "Simulating guitar distortion circuits using wave digital and nonlinear state-space formulations," in *Proc. Int. Conf. Digit. Audio Effects*, Espoo, Finland, Sep. 2008, pp. 19–26.
- [22] R. C. D. Paiva, J. Pakarinen, V. Välimäki, and M. Tikander, "Real-time audio transformer emulation for virtual tube amplifiers," *EURASIP J. Adv. Signal Process.*, vol. 2011, pp. 1–15, 2011.
- [23] R. Boylestad and L. Nashelsky, *Electronic Devices and Circuit Theory*, 8th ed. Englewood Cliffs, NJ: Prentice-Hall, 2002.
- [24] T. C. Banwell and A. Jayakumar, "Exact analytical solution for current flow through diode with series resistance," *Electron. Lett.*, vol. 36, no. 4, pp. 291–292, Feb. 2000.
- [25] D. Veberic, Having fun with Lambert $W(x)$ function, GAP-2009-114. [Online]. Available: <http://arxiv.org/abs/1003.1628>
- [26] LTSpice IV. [Online]. Available: <http://www.linear.com/ltspice>
- [27] A. Farina, "Simultaneous measurement of impulse response and distortion with a swept-sine technique," in *Proc. 108th Audio Eng. Soc. Conv.*, Paris, France, Feb. 2000, Paper 5093.
- [28] J. Pakarinen, "Distortion analysis toolkit—A software tool for easy analysis of nonlinear audio systems," *EURASIP J. Adv. Signal Process.*, vol. 2010, pp. 1–13, Feb. 2010.
- [29] A. Fettweis, "Wave digital filters: Theory and practice," *Proc. IEEE*, vol. 74, no. 2, pp. 270–327, Feb. 1986.
- [30] A. Fettweis and K. Meerkotter, "On adaptors for wave digital filters," *IEEE Trans. Acoust., Speech Signal Process.*, vol. 23, no. 6, pp. 516–525, Dec. 1975.